Mineralogy and Petrology (2018) 112 (Suppl 2):S597–S608
https://doi.org/10.1007/s00710-018-0617-4

ORIGINAL PAPER

Geochemistry and origin of the Mirny field kimberlites, Siberia

Aleksey M. Agashev[1] · Shun'ichi Nakai[2] · Ilya V. Serov[3] · Aleksander V. Tolstov[3] · Konstantin V. Garanin[3] · Oleg E. Kovalchuk[3]

Received: 14 November 2017 / Accepted: 3 July 2018 / Published online: 9 July 2018

Abstract

Here we present new data from a systematic Sr, Nd, O, C isotope and geochemical study of kimberlites of Devonian age Mirny field that are located in the southernmost part of the Siberian diamondiferous province. Major and trace element compositions of the Mirny field kimberlites show a significant compositional variability both between pipes and within one diatreme. They are enriched in incompatible trace elements with La/Yb ratios in the range of (65–300). Initial Nd isotope ratios calculated back to the time of the Mirny field kimberlite emplacement ($t = 360$ ma) are depleted relative to the chondritic uniform reservoir (CHUR) model being 4 up to 6 εNd(t) units, suggesting an asthenospheric source for incompatible elements in kimberlites. Initial Sr isotope ratios are significantly variable, being in the range 0.70387–0.70845, indicating a complex source history and a strong influence of post-magmatic alteration. Four samples have almost identical initial Nd and Sr isotope compositions that are similar to the prevalent mantle (PREMA) reservoir. We propose that the source of the proto-kimberlite melt of the Mirny field kimberlites is the same as that for the majority of ocean island basalts (OIB). The source of the Mirny field kimberlites must possess three main features: It should be enriched with incompatible elements, be depleted in the major elements (Si, Al, Fe and Ti) and heavy rare earth elements (REE) and it should retain the asthenospheric Nd isotope composition. A two-stage model of kimberlite melt formation can fulfil those requirements. The intrusion of small bodies of this proto-kimberlite melt into lithospheric mantle forms a veined heterogeneously enriched source through fractional crystallization and metasomatism of adjacent peridotites. Re-melting of this source shortly after it was metasomatically enriched produced the kimberlite melt. The chemistry, mineralogy and diamond grade of each particular kimberlite are strongly dependent on the character of the heterogeneous source part from which they melted and ascended.

Keywords Kimberlite · Geochemistry · Sr-Nd isotopes · Lithospheric mantle · Siberia

Introduction

Kimberlites are known as incompatible elements and volatile enriched rocks which contain diamond and are derived from deeper levels in the mantle than any other magma. Hence, kimberlite compositions are an important source of information regarding deep mantle compositions and melt-generation processes. Early studies have shown that basaltic and micaceous varieties of Southern African kimberlites differ in their isotopic and geochemical character, and they are thus divided into Groups I and II, respectively (Smith 1983; Smith et al. 1985). The chemical and isotopic contrasts between the two groups are believed to reflect the different compositions of their mantle source regions. Lithophile trace element ratios in Group I (Gr I) kimberlites are generally similar to those of oceanic island basalts (Smith et al. 1985). They also have relatively high initial $^{143}Nd/^{144}Nd$ isotope ratios and low initial $^{87}Sr/^{86}Sr$ ratios compared to Group II kimberlites. The origin of Gr I kimberlites from the convectively mixed (asthenospheric) mantle is generally accepted, but the position of the source remains in question. Opinions are divided between a site just below cratonic lithosphere, and one within a

Editorial handling: A. Giuliani

Electronic supplementary material The online version of this article (https://doi.org/10.1007/s00710-018-0617-4) contains supplementary material, which is available to authorized users.

✉ Aleksey M. Agashev
agashev@igm.nsc.ru

[1] V.S. Sobolev Institute of Geology and Mineralogy, Koptyuga pr.-3, Novosibirsk 630090, Russia

[2] Earthquake Research Institute, The University of Tokyo, Yayoi 1-1-1, Bunkyo-ku, Tokyo 113-0032, Japan

[3] ALROSA Co Ltd., Lenina st. 6, Mirny 678174, Russia

transitional zone between the upper and lower mantle (Smith 1983; Ringwood et al. 1992; Taylor et al. 1994; Tappe et al. 2014). Isotopic signatures of orangeites (Group II kimberlites) indicate an origin from melting of a source within the lithospheric mantle that is characterized by a long-term time-integrated enrichment in incompatible elements (Smith 1983; Tainton and McKenzie 1994; Taylor et al. 1994; Giuliani et al. 2015). The tectonic trigger for kimberlite melting is also debated. Mantle plumes (Haggerty 1994; Torsvik et al. 2010) or only heat and volatiles from plumes or hotspots (Le Roex et al. 2003; Becker and Le Roex 2006) can trigger kimberlite melting. An alternative trigger is volatile supply from the deeply subducted oceanic crust far away from the continent boundary (Duke et al. 2014). Recently Tappe et al. (2014, 2017) argued that kimberlitic melt extraction and transport to the Earth's surface occurred mainly during the fast and changing plate motions that occur during the assembly and breakup of supercontinents.

Previous studies have shown that the Middle Paleozoic kimberlites from the Siberian Platform are isotopically and geochemically similar to South African basaltic kimberlites (Agashev et al. 2000; Kostrovitsky et al. 2007) and can be classified as Gr I rocks. However, the Nakyn field kimberlites of the Siberian craton (Agashev et al. 2001) have unique trace element signatures and Sr and Nd isotope compositions that distinguish them from any other kimberlites worldwide.

Here, we present new data relating to systematic isotope geochemical studies of all kimberlites within the Mirny field which are known for their world class diamond mines first of all Mir and Inter pipes. The geochemical composition of kimberlites is very heterogeneous even between closely located pipes and even within one kimberlite body (Agashev et al. 2000). However, kimberlites composing one kimberlite field could be genetically related and formed by a single tectono-magmatic episode from a single source. In this study, we attempt to find the regularities in the variations of the geochemical compositions of kimberlites within one kimberlite field which could have arisen from such a genetic relationship.

Geological background

The Mirny kimberlite field is located in the southernmost part of the Siberian kimberlite province (Fig. 1), within the Botuobinskaya anticlinal structure, near the western edge of Vilyui Rift Basin (Kiselev et al. 2014). The Archean crystalline basement in this area is covered by an approximately 1.5–2 km thick sequence of sedimentary rocks. The sedimentary sequence consists of carbonate rocks of Cambrian, Ordovician, and upper Silurian age. Those carbonates are partly covered with stratigraphic unconformity by upper Paleozoic and Mesozoic, mostly lower Jurassic, terrigenous rocks with conglomerates and unsorted sandstones as the basal layers. The latter basal rocks often contain diamond and diamond indicator minerals such as pyrope garnets and picroilmenites, suggesting considerable erosion of the kimberlite material after emplacement until Jurassic time.

The major regional deep fault zones have a submeridional direction (Fig. 1). They are traced by magnetic field anomalies and mafic dyke systems. The dykes, which are represented by dolerites, are part of Devonian age dyke swarm along the northwestern shoulder of the Vilyui Rift system (Kiselev et al. 2014). The peripheral faults with a northwest direction are connected with the major fault zones and are traced by a long axis of elongated surface planes of explosion pipes and shear zones in lower Paleozoic sediments. The kimberlite pipes were emplaced at the intersections of the major regional faults with peripheral faults. Some pipes are exposed at the present day surface. Others are covered by thin layers (5–20 m) of lower Jurassic sediments. The emplacement age determined for four Mirny field kimberlite pipes are in range of 356–364 Ma (Davis et al. 1980; Agashev et al. 2016).

Presently in the Mirny field, six kimberlite pipes are known: Mir, Inter, 23 CPC, Amakinskaya, Taezhnaya and Dachnaya. In addition, there are one satellite pipe (Sputnik), two separate dykes (Anomaly 21 and Yuzhnaya), and several dykes connected with the pipes. Hence, the Mirny kimberlite filed is a suitable object to study systematically the compositional variations of kimberlites composing the field. The Inter kimberlites are of very high diamond grade. Kimberlites of the 23 CPC, Mir and Dachnaya pipes are high to middle diamondiferous, The Taezhnaya pipe is sub-economic and the Amakinskaya pipe is poor in diamond (Table 1). At present diamond mines of the Mirny field were mined out; therefore it is difficult to establish the internal structure of the pipes. The Mirny field kimberlites are composed mostly of one (Dachnaya, Amakinskaya, 23 CPC, Anomaly 21) or two (Inter, Taezhnaya) phases of intrusion. The Mir pipe has a more complex structure and six phases of intrusion were identified (Vladimirov et al. 1981), with most of the pipe volume composed of kimberlite breccias.

Samples and analyses

Description of samples, petrography and mineralogy

The Mirny field kimberlites are variably altered by surface processes and their olivine is fully serpentinised; only some of the olivine in the Mir pipe porphyric kimberlite has survived. All kimberlites, including that of the Mirny field, are petrographically complex rocks with three main components. The first two are xenoliths of the mantle and continental crust and a suite of macrocrysts and xenocrysts which is mostly of mantle origin. Olivine macrocrysts are common for all of the Mirny kimberlites and occupy from 15 vol% up to 40 vol% of the rocks. The xenocrysts suite includes the following

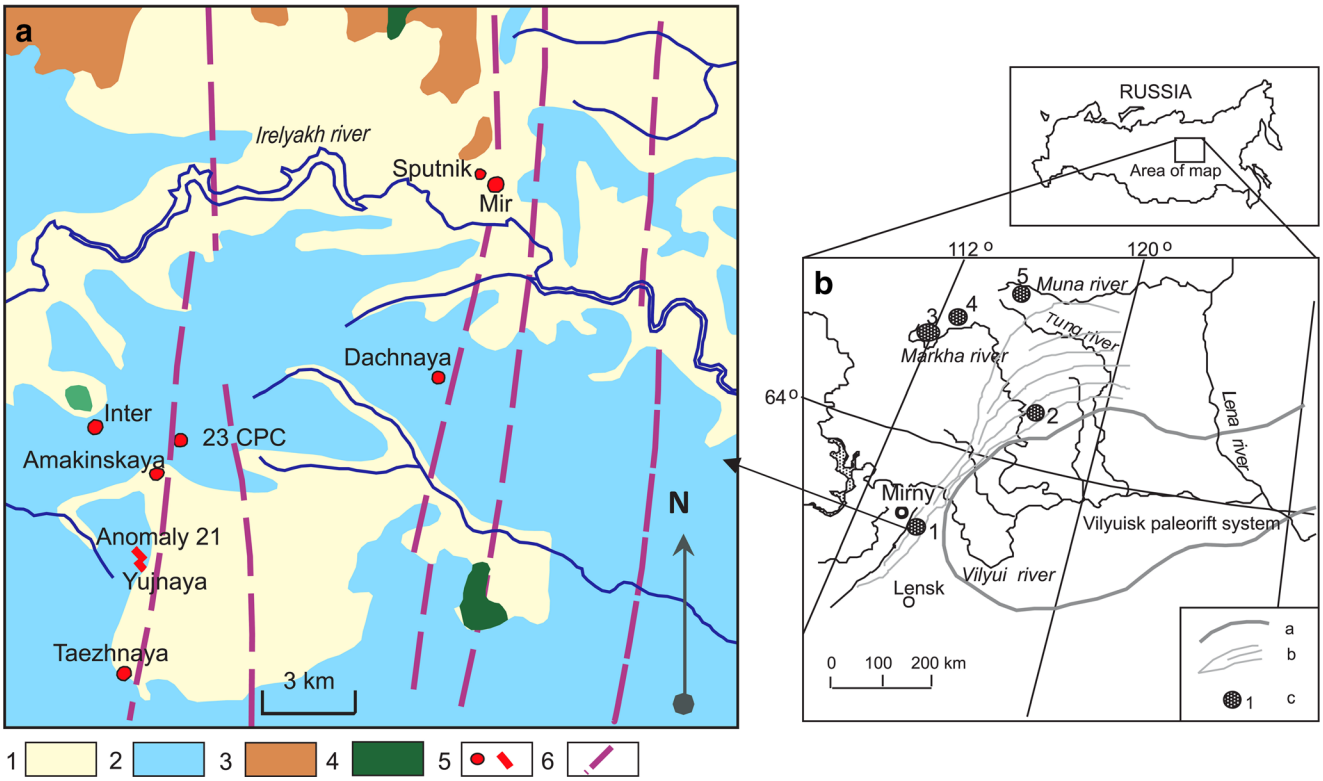

Fig. 1 **a** Simplified geological map of the Mirny kimberlite field. 1 = Upper Cambrian sediments; 2 = Permian sediments; 3 = Lower Jurassic terrigenous sedimentary rocks; 4 = Doleritic intrusions; 5 = Kimberlite bodies; 6 = Regional faults. **b** Map of the Siberian platform showing locations of Middle-Paleozoic kimberlite fields. a = Vilyuisk paleorift system; b = Vilyui-Markha deep fault zone; c = Kimberlite fields (1 = Mirny field; 2 = Nakyn; 3 = Alakit; 4 = Daldyn; 5 = Muna)

minerals: olivine, garnet, chrome-diopside, ilmenite, Gr-spinel, enstatite, phlogopite and diamond. All of these reside in the third componend that consists of a fine grained matrix which is belived to represent the kimberlite itself. The matrix is composed of different proportions of secondary serpentine and calcite and microphenocrysts of olivine, phlogopite, calcite and one or several of the following minerals in small amount(s): apatite, dolomite, diopside, monticellite, spinel, perovskite and ilmenite. Kimberlite samples of this study (0.5–1 kg) were crushed into 3–5 mm chips and ~100 g of fragmens free of xenogenic material were powdered for whole-rocks analysis.

Table 1 Main features of the Mirny field kimberlites

Name	Kimberlite type	Olivine macrocrysts (vol%)	Crustal xenoliths (vol%)	xenocrysts			Pipe size** (ha)	Diamond grade (Ct/t)
				Ilmenite	Ti-rich garnet*(%)	Cr-rich spinel		
Inter	Porphyric kimberlite	20–45	0–5	trace	<5	high	1.27	9
23 CPC	Kimberlite breccia	15–40	10–20	trace	3.6	high	0.2	3–4
Mir	Porphyric kimberlite	20–40	0–5	moderate	moderate	moderate	12.33	4–5
Mir	Kimberlite breccia	15–30	5–20	high	9.4	moderate	12.33	4–5
Dachnaya	Kimberlite breccia	15–40	15–20	high	7.3	moderate	0.3	1.7
Taezhnaya	Porphyric kimberlite	20–40	0–10	high	9.6	low	0.15	0.23
Taezhnaya	Aphyric kimberlite	0–5	0–5	high	n.d.	trace	0.15	n.d
Amakinskaya	Kimberlite breccia	15–30	10–30	very high	13.3	trace	2.5	0.05
Anomaly 21	Aphyric kimberlite	0–5	0–5	high	n.d.	trace		0.2

Abundance of olivine macrocrysts and crustal xenoliths were evaluated by visual examination of rock samples and thin-sections. Relative abundances of xenocrysts were evaluated by inspection of heavy minerals concentrates

* Fraction of low Cr, Ti-rich megacrysts among the total number of garnet xenocrysts studied

** Surface squares of pipes

Samples of Mirny field kimberlites are represented by three petrographic types. Porphyritic kimberlite (PK) that has abundunt serpentinised olivine macrocrysts set in a fine grained matrix and corresponds to the hypabyssal facies kimberlites of textural genetic classification (Clement and Skinner 1985). Kimberlite breccias (KB) which has abundunt xenoliths that are mostly fragments of wall-rock sediment, and Aphyric kimberlie (AK) that contains very little xenoliths or xenocrysts. The petrographic type of every studied sample, along with the sampling sites, is provided in Table S1 (Electronic Supplementary Material). The study of heavy mineral concentrates reveals significant differences in the abundances of mantle-derived ilmenite, Cr-poor Ti rich garnets and Cr-rich spinel xenocrysts between the different Mirny field kimberlites. Randomly selected garnet xenocryst fractions (100–200 grains) were studied for chemical composition (Aleksey A. Agashev and co-workers, unpublished data) and proportion (in % out of total number of grains studied) of Ti-rich Cr- poor garnet was calculated. A summary of the main features of the Mirny field kimberlite petrographic types along with their abundances of olivine macrocrysts and xenoliths of mostly upper crust sediments as well as their relative abundances of mantle-derived xenocrysts is provided in Table 1. The average diamond grade and the surface sizes of the pipes are also shown. The relationship between kimberlite chemistry (average TiO_2 contents), abundances of Ti-rich Cr- poor garnet xenocrysts and diamond grade are presented in Fig. 2. The chemical compositions of those garnet xenocrysts are given in the Electronic Supplementary Material.

Analytical methods

Major oxides in whole rock samples were measured by X-ray fluorescence (XRF) analysis using an ARL–9900 XP spectrometer. Trace element concentrations in the rocks were determined on a Finnigan MAT ELEMENT high-resolution inductively coupled plasma mass spectrometer (ICPMS) with a U-5000AT+ ultrasonic nebulizer. Samples were digested using the method of Li metaborate fusion followed by dissolution (Nikolaeva et al. 2008). The quality of trace elements determinations was controlled by the SARM-39 international kimberlite standard (see Electronic Supplementary Material). The isotopic compositions of oxygen and carbon were measured with a Finnigan MAT-253 mass spectrometer with sample preparation on a Gas Bench II line by standard methods. The accuracy of the carbon and oxygen carbonate material measurements was controlled by the NBS19 international standard ($\delta^{13}C_{VPDB} = +1.9‰$, $\delta^{18}O_{VSMOW} = -2.2‰$) and was 0.1‰ for $\delta^{13}C$ and $\delta^{18}O$ values.

The Rb-Sr and Sm-Nd isotopic compositions were determined on a GV instruments IsoProbe multi-collector (MC) ICPMS. Strontium and Nd were purified using Sr-SPS resin (SR-B25-S, 50–100 mesh; Eichrom Technologies Inc.) and Ln resin (LN-B25-S, 50–100 mesh; Eichrom Technologies Inc.) following the method described by Nishio et al. (2004). The $^{87}Sr/^{86}Sr$ and $^{143}Nd/^{144}Nd$ data were normalized to $^{87}Sr/^{86}Sr = 0.710258$ for SRM987 and to $^{143}Nd/^{144}Nd = 0.5121067$ for JNdi-1. The results of the standard rock analyses are as follows; $^{143}Nd/^{144}Nd = 0.513054 \pm 10$ for JB3 and $^{87}Sr/^{86}Sr = 0.703776 \pm 12$ JB2. Decay constant of $^{87}Rb = 1.42 \times 10^{-11}$ a^{-1} and for $^{147}Sm = 6.54 \times 10^{-12}$ a^{-1} were used for initial isotope ratios calculations. Calculations of the εNd(t) values are based on the compositions of CHUR $^{143}Nd/^{144}Nd = 0.512638$ and $^{147}Sm/^{144}Nd = 0.1967$ (Faure 1986).

Results

Chemical compositions

Major elements

Analytical data regarding major and trace element compositions are provided in the Electronic Supplementary Material along with replicate analyses of the SARM-39 kimberlite standard. As can be seen from Fig. 2, the Mirny field kimberlites show a significant compositional variability both between pipes and within one diatreme, which is typical for kimberlites. Most of the compositional variability is represented by the negative covariation of SiO_2 and MgO with CaO contents (Fig. 2), which reflects the proportions of silicate (olivine-serpentine) and carbonate within the rocks. The variability in the abundances of phlogopite and ilmenite results in variability in the K_2O and TiO_2 contents. Based on the major elements, the Mirny field kimberlites can be rougly divided in three varieties. The first variety is represented by Inter and 23 CPC kimberlites which have low TiO_2 and Fe_2O_3 contents that vary in the range 0.38–0.77 wt% and 2.74–7.05 wt% respectively. The second variety, which includes rocks of the Mir, Dachnaya and Taezhnaya pipes, is of intermediate composition and contains 0.75–1.78 wt% of TiO_2 and 6.43–10.94 wt% of Fe_2O_3. The last group is a high Ti variety that includes kimberlites of the Amakinskaya pipe, aphyric kimberlite of the Taezhnaya pipe and rocks of the Anomaly 21dyke. Low Ti kimberlites are characterized by a significant amount of phlogopite in their groundmass and a small amount of ilmenite macrocrysts. The high Ti variety, in turn, contains a significant amount of ilmenite.

The relationship between the TiO_2 and K_2O contents also provides an important distinction between Gr I kimberlites and orangeites (Smith et al. 1985). Most of the Mirny field kimberlites plot within the field of the South African Gr I kimberlite (Fig. 2), which is in agreement with their major element composition. The compositions of the Inter and 23 CPC pipes plot at the low concentration corner of the orangeites; however, the K_2O content in the kimberlites of

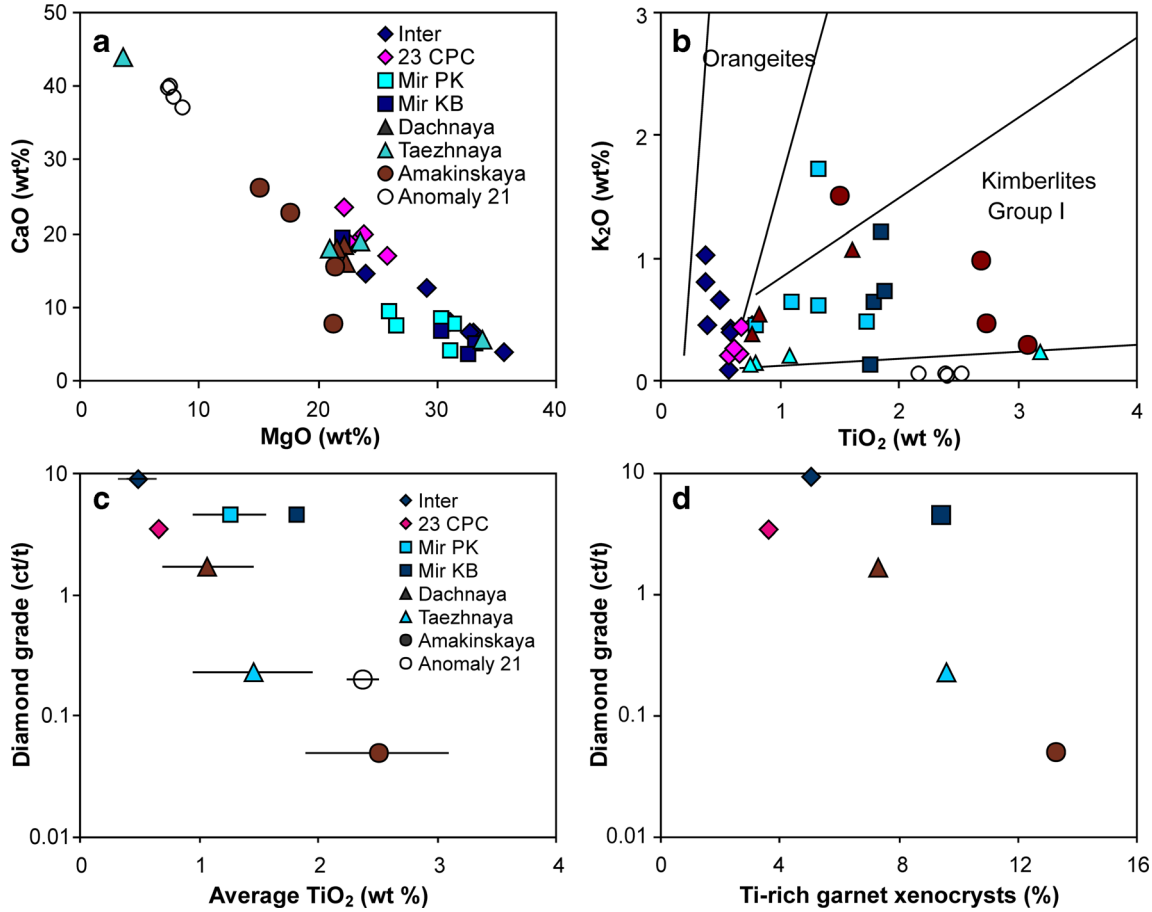

Fig. 2 **a** MgO-CaO and **b**) K_2O-TiO_2 relations diagrams for the Mirny field kimberlites composition. Fields of kimberlites Gr I and orangeites after Smith et al. (1985). **c** Diamond grade vs average TiO_2 contents in kimberlites, lines are standard deviation. **d** Diamond grade vs abundances of Ti-rich Cr poor garnets xenocrysts in % from total number of garnet xenocrysts studied

these pipes (0.8 wt%) is significantly lower than the average of the orangeites (3.3 wt%) of South Africa.

Trace elements

Kimberlites of the Mirny field are enriched in incompatible trace elements [Ba, Sr, Nb, Ta, Zr, Hf, Th, U and light REE (LREE)]. The degree of enrichment in incompatible elements is variable between and within particular pipes and the concentrations of LIL (Rb, Ba, and K) elements are the most variable. Variation in the concentrations of LREE and high field strength elements (HFSE) in the Mirny field kimberlites are also significant but to a lesser degree than those of large-ion lithophile elements (LILE). For example, the range of REE fractionation among the samples of one pipe expressed as La/Yb ratio could be very high (124–270) for the Inter pipe. Porphyritic kimberlite and kimberlite breccia of the Mir pipe are clearly different in trace element concentrations and ratios. Porphyritic kimberlite contains less of the incompatible elements and has a low La/Yb ratio (62–105) compared to KB (156–300). In spite of the high variations in the absolute concentrations of incompatible elements, the average compositions of the Mirny field kimberlites are very similar on log-scale primitive mantle (PM) normalized spidergrams (Fig. 3). The only clear difference is the Ti anomaly that is negative in the low Ti kimberlites and positive in the high Ti kimberlites. Concentrations of the incompatible elements normalized to the PM composition (Fig. 3) have negative anomalies for Rb, K, Zr and positive ones for Nb, Th, Ba, Nd and Sm. This type of distribution has been shown to be common for Gr I kimberlites (Smith et al. 1985) and plume-related OIB. Indicative trace element ratios of the Mirny kimberlites are Nb/Zr >1 and La/Nb <1, which are typical for kimberlites of Gr I. On the plot of Ba/Nb and La/Nb ratios, the Mirny field rocks are similar to Gr I kimberlites and show scatter in their Ba/Nb ratios along the composition of main mantle reservoirs (Weaver 1991) from values lower than that of OIB originated from source with high U/Pb ratio (HIMU) and up to values of OIB originated from enriched mantle source (EM) (Fig. 4).

Sr-Nd isotopes

Initial Nd isotope ratios calculated back to time of the Mirny field kimberlite emplacement ($t = 360$ Ma,

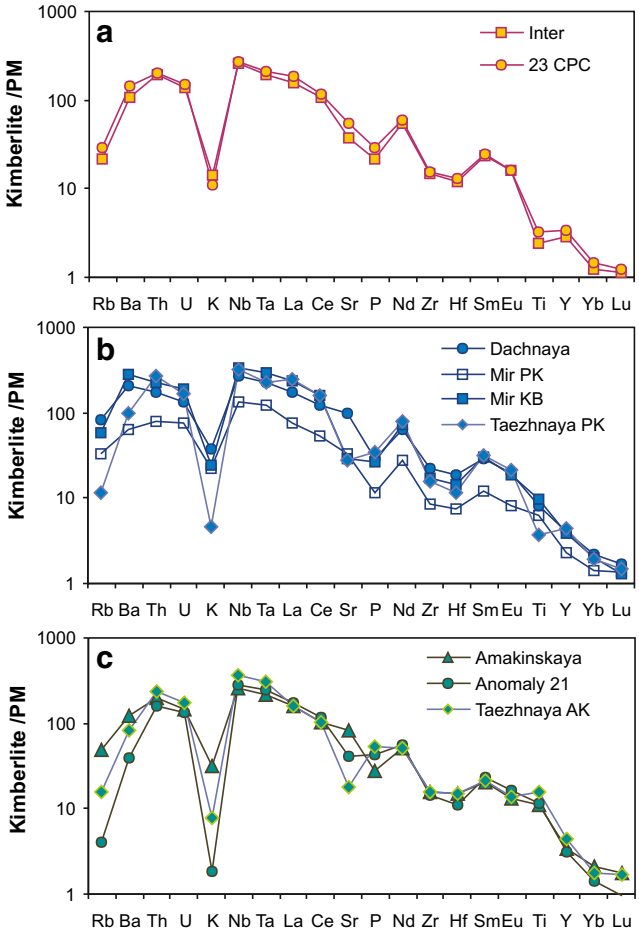

Fig. 3 Primitive Mantle (PM) normalized trace elements patterns of the Mirny field kimberlites. PM values after McDonough and Sun (1995)

Agashev et al. 2016) show variable depletion relative CHUR model being 4 up to 6 εNd(t) units (Table 2 and

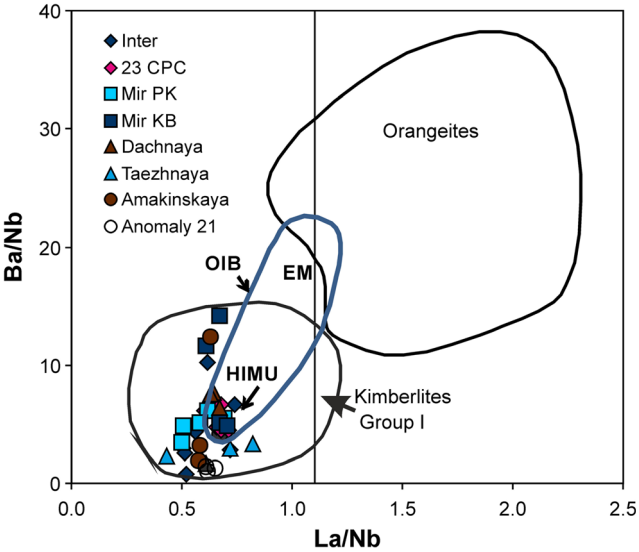

Fig. 4 La/Nb vs Ba/Nb ratios diagram for the Mirny field kimberlites. Compositional fields for MORB and OIB after Weaver (1991) and Willbold and Stracke (2006)

Fig.5). Given their Sr and Nd isotope compositions, these kimberlites could be classified as Gr I, as is the case for most of the Siberian middle-Paleozoic kimberlites (Agashev et al. 2000; Kostrovitsky et al. 2007) but they are clearly different from the Nakyn kimberlites of Siberia (Agashev et al. 2001) and the orangeites of South Africa (Smith et al. 1985; Giuliani et al. 2015). Initial Sr isotope ratios are significantly variable, being in the range of 0.70387 to 0.70845. Increases in initial Sr isotope ratios in the Mirny field kimberlites are accompanied by slight decreases of εNd(t) values. Four samples have almost identical Nd and Sr isotope compositions with εNd(t) values of 5.64–5.96 and initial $^{87}Sr/^{86}Sr$ ratios of 0.70387–0.70408. Two of these samples are from the 23 CPC pipe, one is from the Taezhnaya pipe and one from Anomaly 21, all together they closely correspond to the PREMA (Prevalent Mantle) composition of the Zindler and Hart (1986) definition. Previously reported Sr-Nd isotope compositions of the Siberian kimberlites (Agashev et al. 2000; Carlson et al. 2006) also show spread towards radiogenic Sr composition at positive εNd(t) values, with the exception of the Devonian Nakyn field kimberlites (Agashev et al. 2001) which have a distinct Nd isotope composition with εNd(t) values of around 0 (Fig. 4). Sun et al. (2014) reported a number of in situ Sr-Nd isotope analyses of perovskites from Siberian kimberlites but none however from the Mirny field. These perovskite data show a rather narrow range of initial Sr isotope composition (0.7028–7038) with variable εNd(t) values from 2 to 6.

O and C isotopes

The $\delta^{13}C_{VPDB}$ values of the carbonate components of the Mirny field kimberlites (Table 3) vary between −4.6 and −9.8‰. This mostly corresponds to the mantle carbon composition (Deines 2002), with the samples from Anomaly 21 having slightly lower values (Fig. 6a). Oxygen isotope compositions are outside of the range of mantle carbonates, being higher, and vary between 16.3 and 26‰ $\delta^{18}O_{VSMOW}$. This high variation of oxygen isotope composition in a narrow range of carbon isotope compositions is common for kimberlites (Giuliani et al. 2014).

Discussion

Source of protho-kimberlite melt

Four samples have almost identical initial Nd and Sr isotope compositions that are similar to the PREMA reservoir of Zindler and Hart (1986), suggesting an asthenospheric source for the incompatible elements in

Table 2 Rb-Sr and Sm-Nd isotope composition of the Mirny filed Kimberlites

Pipe	Sample	Rb (ppm)	Sr (ppm)	$^{87}Rb/^{86}Sr$	$^{87}Sr/^{86}Sr$	2SE	$^{87}Sr/^{86}Sr(t)$
Inter	In71	11.86	238.1	0.1441	0.709201	±31	0.708450
Inter	In74	19.74	561.0	0.1018	0.705654	±20	0.705124
Inter	In75	2.03	263.6	0.0223	0.707192	±18	0.707076
23 CPC	Ps72	14.44	912.7	0.0458	0.704240	±25	0.704002
24 CPC	Ps73	26.68	1321.4	0.0584	0.704237	±17	0.703932
Mir	M4	9.44	286.3	0.0954	0.706970	±18	0.706473
Mir	M29	33.51	523.6	0.1851	0.706095	±25	0.705130
Mir	M58	8.86	627.3	0.0409	0.707560	±16	0.707346
Taezhnaya	Tj74	9.62	356.4	0.0781	0.707020	±23	0.706613
Taezhnaya	Tj75	6.33	507.3	0.0361	0.704058	±20	0.703870
Amakinskaya	Am 19/55	15.54	867.3	0.0518	0.708006	±23	0.707735
Anomaly 21	An27	1.85	364.8	0.0147	0.707109	±17	0.707032
Anomaly 21	An32	2.67	1320.3	0.0058	0.704115	±20	0.704084
		Nd (ppm)	Sm (ppm)	$^{147}Sm/^{144}Nd$	$^{143}Nd/^{144}Nd$	2SE	εNd(t)
Inter	In71	38.91	5.43	0.0843	0.512620	±10	4.91
Inter	In74	53.7	7.04	0.0792	0.512653	±11	5.79
Inter	In75	82.38	10.83	0.0794	0.512641	±9	5.54
23 CPC	Ps72	73.4	9.4	0.0774	0.512639	±8	5.60
23 CPC	Ps73	76.42	10.02	0.0793	0.512646	±9	5.65
Mir	M4	117.39	12.85	0.0661	0.512586	±8	5.09
Mir	M29	85.98	10.88	0.0765	0.512564	±9	4.18
Mir	M58	27.34	3.78	0.0835	0.512606	±10	4.67
Taezhnaya	Tj74	64.97	8.65	0.0805	0.512567	±9	4.05
Taezhnaya	Tj75	99.63	13.16	0.0798	0.512647	±9	5.64
Amakinskaya	Am 19/55	91.77	11.85	0.0781	0.512552	±11	3.87
Anomaly 21	An27	69.79	10.06	0.0872	0.512638	±10	5.12
Anomaly 21	An32	76.87	10.2	0.0802	0.512664	±10	5.96

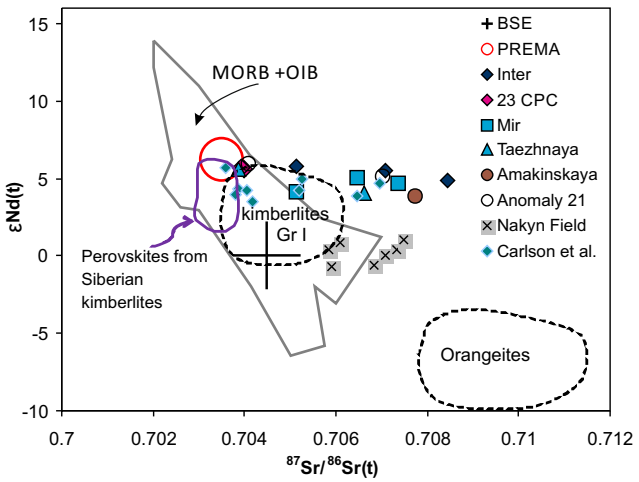

Fig. 5 Sr and Nd isotope composition of the Mirny field kimberlites. Compositional fields for MORB and OIB after Hofmann (1997). Nakyn field kimberlites after Agashev et al. (2001). Kimberlites Group I and orangeites after Smith (1983). Siberian kimberlite data of Carlson et al. (2006) is also shown. Data on perovskites composition after Sun et al. (2014). Bulk silicate earth (BSE) after Faure (1986)

kimberlites. Prevalent mantle is the most common isotopic signature for OIB. We can propose that the source of proto-kimberlite melt of the Mirny field kimberlites is the same as for the majority of OIB. This is supported by the ratios of very incompatible elements that do not fractionate in partial melting and crystallization processes such as La/Nb, Nb/U, U/Th, which are OIB like in the Mirny field kimberlites. The shift towards radiogenic Sr isotope ratios could result from a combination of several reasons. Theoretically, it could be the assimilation of old enriched material within the lithospheric mantle, such as K-rich metasomes (Rosenthal et al. 2009). Peridotites at the base of lithospheric mantle also keep the sign of old metasomatism, thus deformed peridotites of the Udachnaya kimberlite have initial Sr isotope ratios up to 0.7055 (Surgutanova et al. 2016). Radiogenic Sr is also reported to be part of diamond forming fluid (Klein-BenDavid et al. 2014). Secondly, it could be contamination of kimberlites by wall rocks that contain carbonates and evaporates (Kostrovitsky et al. 2007; Kopylova et al. 2013). As is

Table 3 O and C isotope composition of the Mirny field kimberlites

Pipe	Sample	$\delta^{13}C_{VPDB}$(‰)	$\delta^{18}O_{VSMOW}$(‰)
Inter	In71	−5.5	26
Inter	In74	−4.7	16.4
Inter	In75	−6.2	23.2
23 CPC	Ps72	−6.1	16.3
24 CPC	Ps73	−4.6	16.7
Mir	M4	−5.7	23.4
Mir	M29	−7.2	23.6
Mir	M58	−6.4	15
Taezhnaya	Tj74	−5.5	17.3
Taezhnaya	Tj75	−8.6	18.4
Amakinskaya	Am 19/55	−5	21.3
Anomaly 21	An27	−9.8	14
Anomaly 21	An32	−9	14.9

shown by Agashev et al. (2000), simple mechanical mixing with carbonate sediment through which the Siberian kimberlites were intruded could not explain the elevated Sr isotope ratios of these kimberlites as it requires up to 50 % sediments addition. Sample preparation carefully removed any visible entrained crustal xenogenic material before making powders to exclude this possibility. The most probable reason for increase of Sr isotope ratio is the post-magmatic ground water circulation and its exchange of Sr with the kimberlites (Woodhead et al. 2009; Giuliani et al. 2014, 2017). The radiogenic Sr isotope tends to be positively correlated with oxygen isotope composition, which could support a post-magmatic hydrothermal process as a reason for the elevated Sr isotope composition (Fig. 6b). The increase of $\delta^{18}O$‰ at nearly constant $\delta^{13}C$‰ is usually explained by deuteric fluid circulation (Wilson et al. 2007) or by hydrothermal post-magmatic processes (Deines 1989; Giuliani et al. 2014). Three samples have low $\delta^{13}C$ values and their O-C isotope composition is consistent with carbonate crystallization after extensive CO_2 degassing (Demeny et al. 1998; Giuliani et al. 2014). Samples with lower concentrations of Sr could be more easily affected by secondary alteration processes as their Sr isotope composition is negatively correlated with Sr content.

Kimberlite source formation and melting

Based on the chemical composition and mineralogy, kimberlites of the Mirny field could be subdivided into 3 groups. The first group represents the kimberlites of Inter and 23 CPC, which have low TiO_2 and Fe_2O_3 contents and are very similar to each other in geochemical composition. They contain little ilmenite and other minerals of the low Cr megacrysts suite and are very rich in diamond. The second group includes the Mir, Dachnaya and Taezhnaya pipes. The Mir kimberlite pipe is one of the world biggest diamond deposits and consists of two main varieties of kimberlites (PK and KB), which systematically differ in their geochemical compositions. The KB is enriched in all incompatible elements compared to PK, indicating that these two types of kimberlites within one pipe are derived from a different batch of magma. Kimberlites of the Dachnaya and Taezhnaya pipes are

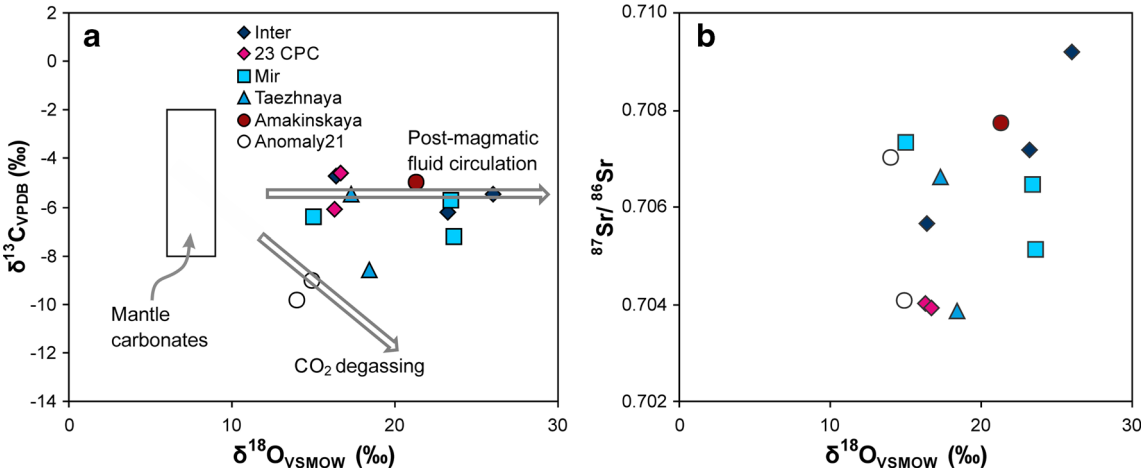

Fig. 6 **a** O and C isotope composition of the Mirny field kimberlites. The mantle carbonate compositional box is from Giuliani et al. (2014) the trends of post-magmatic fluid circulation and CO_2 degassing after (Demeny et al. 1998; Giuliani et al. 2014). **b** Relationship between Sr and O isotope composition of the Mirny field kimberlites

compositionally very similar to KB of the Mir pipe. Kimberlites of the Amakinskaya pipe contain a high amount of low Cr megacrysts, have a low diamond grade and are enriched in TiO_2 and HFSE relative to light and middle REE. AK of Anomaly 21 dyke and the Taezhnaya pipe are TiO_2 rich and contain little diamond.

It is very improbable that all of the compositional variability of the Mirny field kimberlites has arisen from the assimilation and contamination of lithospheric mantle material and fractionation of the melt that formed in the asthenosphere below. In this case, the composition of the kimberlites would be more or less similar to each other. However within the pipes compositional variabily could be resulted from differen degress of interaction with peridotitic rocks during ascent (Giuliani et al. 2016). The source of the Mirny field kimberlites has to combine three main features. It should be enriched in incompatible elements over PM, be depleted in major elements (Si, Al, Fe and Ti) and heavy REE and it should retain the asthenospheric Nd isotope composition. The base of the lithospheric mantle metasomatised just prior to kimberlite melting and fulfills all of these requirements (Agashev et al. 2006). Therefore, we consider that a two-stage model of kimberlite melt formation (Tainton and McKenzie 1994; Agashev et al. 2000, 2008; Yaxley et al. 2017) is more plausible to explain the great variation of kimberlite chemistry and their diamond contents. Geochemical variations in kimberlite composition within one field could be explained by a combination of factors and first of all is the small-scale heterogeneity of the source. The formation of an incompatible element enriched source for the kimberlites is initiated by intrusion into the lithospheric mantle of small bodies of proto-kimberlite melt that formed within the convecting mantle of a PREMA-like composition. Magmas ascending from the asthenosphere beneath could form the veined heterogeneously enriched source through fractional crystallization and metasomatism of adjacent peridotites. There could be two main types of source enrichment; high-temperature silicate matasomatism and lower-temperature metasomatism by residual carbonatite melt. High-temperature silicate metasomatism directly by asthenospheric magmas that make pyroxenite veins and precipitate the low Cr megacrysts suite is not favourable for diamond survival. Residual carbonatite and volatile rich melt percolates away from the pyroxenite veins and makes up an enriched reservoir within peridotites, precipitating minor metasomatic phases and cryptically metasomatise peridotite minerals. This lower-temperature metasomatic process is probably favourable for diamond survival and even grows off of the new crystals. Further supply of heat and volatiles from the asthenosphere below initiate the melting of this enriched source within the lithospheric mantle. The time span between metasomatism by proto-kimberlite melt and formation the kimberlite melt itself could be very short (Agashev et al. 2006). The kimberlite source formation and emplacement events are closely related in time and could be associated to crustal extension in the nearby Vilyui rift system. This relation is in line with Tappe et al. (2014, 2017) proposal that kimberlite magmatism is triggered by major continental reorganisations.

Melting of the veined parts of the source enriched in the low-Cr megacrysts suite could be responsible for the low diamond grade, and Ti and Fe rich kimberlites of the Amakinskaya pipe. Melts for diamond rich kimberlites of the Inter and 23 CPC pipes could be formed from part of a source that experienced low-temperature metasomatism by residual CO_2-rich melt/fluid. A good example of this scenario could be the Inter, 23 CPC and Amakinskaya pipes which are located in close proximity to each other (~3 km). Kimberlite melt of the Amakinskaya pipe could have formed in the metasomatic channel where the asthenospheric melt was crystallized and therefore bring to the surface a set of Ti rich garnet and ilmenite megacrysts and little diamond. Kimberlites of the Inter and 23 CPC pipes were fromed from a source that was peridotite metasomatised by residual melts and fluids at a distance from the channel and have traces of Ti-rich garnet or ilmenite but very diamondiferous. In melting of the high volume kimberlite magma of the Mir pipe, several batches of magma were formed, and probably diverse parts of source were involved and sampled (Fig.7).

The search for a primary melt composition that is common to all kimberlites is useless as every particular kimberlite body formed from their own unique segmet of a heterogeneous source at the base of the lithospheric mantle. In their work, Kjarsgaard et al. (2009) mentioned that at least three different primary kimberlite melts are present among the Lac de Gras kimberlites. However, at the initial stages all kimberlites are more carbonatitic in composition than we see at the surfuce (Agashev et al. 2008; Kamenetsky et al. 2008; Giuliani et al. 2012; Pokhilenko et al. 2015; Bussweiler et al. 2015; Soltys et al. 2016). Only their isotopic compositions of Nd, Hf and unaltered (lowest) Sr isotope values along with their ratios of very incompatible elements that are not fractionated durind melting and crystallization allow us to trace their common asthenospheric OIB-like proto-kimberlite melt composition. The last feature is brodly common for all Gr I kimberlites worldwide

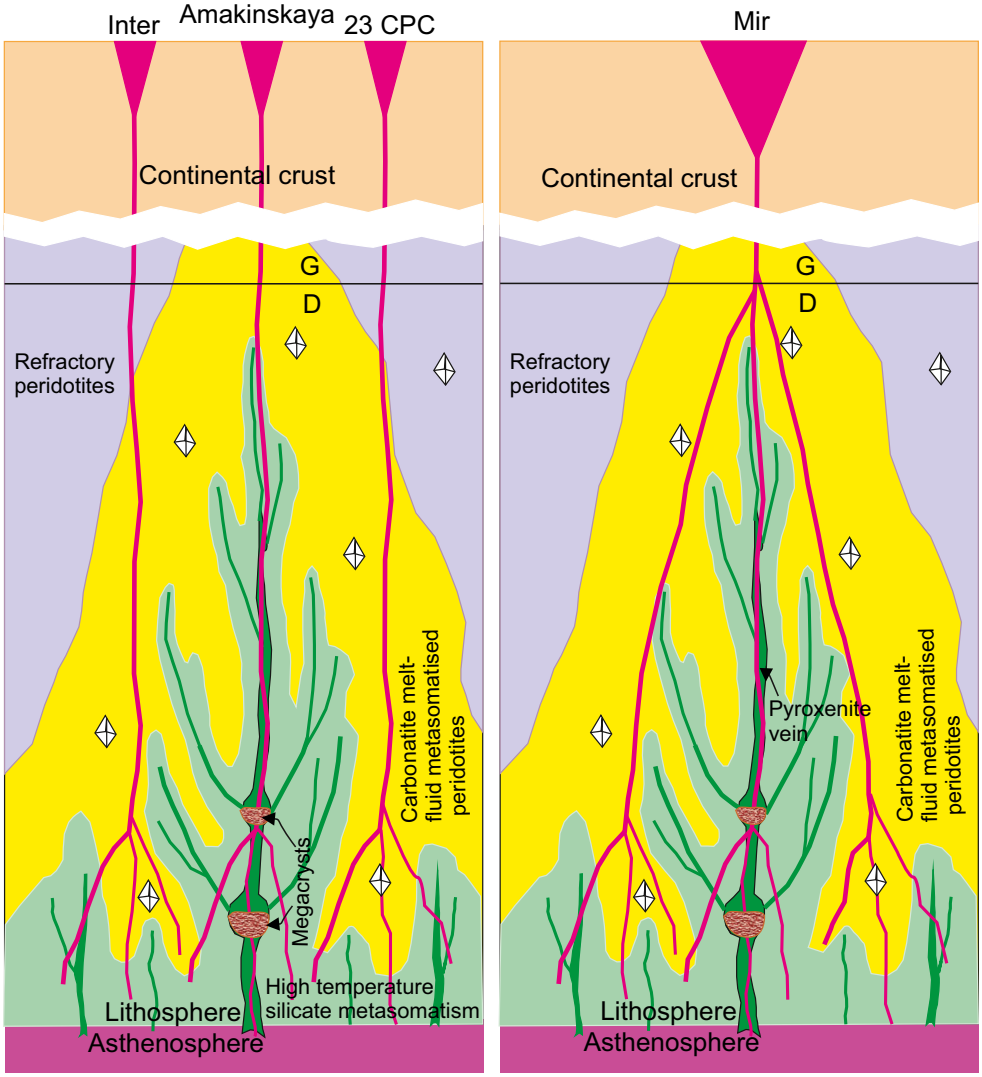

Fig. 7 Simplified model of two stage kimberlite melt formation and emplacement for the Mirny field kimberlites. Proto-kimberlite melt ascending from the asthenosphere could form the veined heterogeneously enriched source. There could be two main types of source enrichment; high-temperature silicate metasomatism (green field) and lower-temperature metasomatism by residual carbonatite melt/fluid (yellow field). The time span between metasomatism by proto-kimberlite melt and formation the kimberlite melt itself (red lines) could be very short. Small volume pipes sampled a single source but high volume Mir pipe probably consists of several batches of magma that sampled a different sources

(Smith 1983; Becker and Le Roex 2006; Nowell et al. 2004; Tappe et al. 2011; Sun et al. 2014).

Conclusions

Mirny field kimberlites have a significant compositional variability both between pipes and within one diatreme which arose from small-scale source heterogenity and different amounts of assimilation and entrainment of mantle material during ascent. Based on their chemical composition and mineralogy, kimberlites of the Mirny field could be subdivided into 3 groups with low, middle and high TiO_2 contents, respectively. These groups also differs in the amout of low-Cr and Ti-rich megacrysts entrained. Proto-kimberlite melts for the Mirny field kimberlites were asthenospheric OIB-like melt from the PREMA-like source. The intrusion of small bodies of this proto-kimberlites melt into the lithospheric mantle forms the veined heterogeneously enriched source through fractional crystallization and metasomatism of the adjacent peridotites. Re-melting of this source shortly after it was metasomatically enriched produced the kimberlite melt. The diamond grade of a particular kimberlite strongly depends on the character of the asthenospheric melt invasion to its source segmets at the base of the lithospheric mantle. Kimberlites that melted along the proto-kimberlite melt channels contain little diamond or are barren whereas kimberlites which have a peridotitic source that were enriched by residual carbonatitic melt or fluids have a greater chance of having an economcal grade of diamond.

Acknowledgements We are grateful to Yuji Orihashi for discussions. Reviews by Montgarry Castillo-Oliver and Larry Heaman greatly helped to improve the manuscript. The editorial handling by Andrea Giuliani and Lutz Nasdala is highly appreciated. The research was supported by the Russian Foundation for Basic Research, grants 15-05-07758a and 16-05-00811a and by state assignment project (project 0330-2016-0006). This work was partially supported by the Earthquake Research Institute of the University of Tokyo Cooperative Research Program.

References

Agashev AM, Orihashi Y, Watanabe T, Pokhilenko NP, Serenko VP (2000) Isotope-geochemical features of the Siberian Platform kimberlites in connection with the problem of their origin. Russ Geol Geophys 41(1):87–97

Agashev AM, Watanabe T, Bydaev DA, Pokhilenko NP, Fomin AS, Maehara K, Maeda J (2001) Geochemistry of kimberlites from the Nakyn field, Siberia: evidence for unique source composition. Geology 29:267–270

Agashev AM, Pokhilenko NP, Malkovetz VG, Sobolev NV (2006) Sm–Nd isotopic system in garnet megacrysts from the Udachnaya kimberlite pipe (Yakutia) and petrogenesis of kimberlites. Dokl Earth Sci 407:491–494

Agashev AM, Pokhilenko NP, Takazawa E, McDonald JA, Vavilov MA, Watanabe T, Sobolev NV (2008) Primary melting sequence of a deep (>250 km) lithospheric mantle as recorded in the geochemistry of kimberlite-carbonatite assemblages, Snap Lake dyke system, Canada. Chem Geol 255:317–328

Agashev AM, Orihashi Y, Pokhilenko NP, Serov IV, Tolstov AV, Nakai S (2016) Age of Mirny field kimberlites (Siberia) and application of Rutile and Titanite for U–Pb dating of kimberlite emplacement by LA-ICP-MS. Geochem J 50:431–438

Becker M, Le Roex AP (2006) Geochemistry of south African on- and off-craton, Group I and Group II kimberlites: petrogenesis and source region evolution. J Petrol 47:673–703

Bussweiler Y, Foley SF, Prelević D, Jacob DE (2015) The olivine macrocryst problem: new insights from minor and trace element compositions of olivine from Lac de Gras kimberlites, Canada. Lithos 220–223:238–252

Carlson RW, Czamanske G, Fedorenko V, Ilupin I (2006) A comparison of Siberian meimechites and kimberlites: implications for the source of high-Mg alkalic magmas and flood basalts. Geochem Geophys Geosyst 7:Q11014

Clement CR, Skinner EMW (1985) A textural genetic classification of kimberlites. Trans Geol Soc S Afr 88:403–409

Davis GL, Sobolev NV, Khar'kiv AN (1980) New data on Yakytian kimberlites age obtained by U–Pb method on zirkons. Dokl Akad Nauk 254(1):175–179

Deines P (1989) Stable isotope variations in carbonatites. In: Bell K (ed) Carbonatites: genesis and evolution. Unwin Hyman, London, pp 301–359

Deines P (2002) The carbon isotope geochemistry of mantle xenoliths. Earth Sci Rev 58:247–278

Demeny A, Ahijado A, Casillas R, Vennemann TW (1998) Crustal contamination and fluid/rock interaction in the carbonatites of Fuerteventura (Canary Islands, Spain): a C, O, H isotope study. Lithos 44:101–115

Duke GI, Carlson RW, Frost CD, Hearn BC Jr, Eby GN (2014) Continent-scale linearity of kimberlite–carbonatite magmatism, mid-continent North America. Earth Planet Sci Lett 403:1–14

Faure G (1986) Principles of isotope geology. Wiley, New York

Giuliani A, Kamenetsky VS, Phillips D, Kendrick MA, Wyatt BA, Goemann K (2012) Nature of alkali-carbonate fluids in the sub-continental lithospheric mantle. Geology 40:967–970

Giuliani A, Phillips D, Kamenetsky VS, Fiorentini ML, Farquhar J, Kendrick MA (2014) Stable isotope (C, O, S) compositions of volatile-rich minerals in kimberlites: a review. Chem Geol 374:61–83

Giuliani A, Phillips D, Woodhead JD, Kamenetsky VS, Fiorentini ML, Maas R, Soltys A, Armstrong RA (2015) Did diamond-bearing orangeites originate from MARID-veined peridotites in the lithospheric mantle? Nat Commun 6:6837

Giuliani A, Phillips D, Kamenetsky VS, Goemann K (2016) Constraints on kimberlite ascent mechanisms revealed by phlogopite compositions in kimberlites and mantle xenoliths. Lithos 240–243:189–201

Giuliani A, Soltys A, Phillips D, Kamenetsky VS, Maas R, Goemann K, Woodhead JD, Drysdale RN, Griffin WL (2017) The final stages of kimberlite petrogenesis: petrography, mineral chemistry, melt inclusions and Sr-C-O isotope geochemistry of the Bultfontein kimberlite (Kimberley, South Africa). Chem Geol 455:342–356

Haggerty SE (1994) Superkimberlites: a geodynamic diamond window to the Earth's core. Earth Planet Sci Lett 122:57–69

Hofmann AW (1997) Mantle geochemistry: the message from oceanic volcanism. Nature 385:219–229

Kamenetsky VS, Kamenetsky MB, Sobolev AV, Golovin AV, Demouchy S, Faure K, Sharygin VV, Kuzmin DV (2008) Olivine in the Udachnaya-east kimberlite (Yakutia, Russia): types, compositions and origins. J Petrol 49:823–839

Kiselev AI, Yarmolyuk VV, Ivanov AV, Egorov KN (2014) Middle Paleozoic basaltic and kimberlitic magmatism in the northwestern shoulder of the Vilyui Rift, Siberia: relations in space and time. Russ Geol Geophys 55(2):185–196

Kjarsgaard BA, Pearson DG, Tappe S, Nowell GM, Dowall D (2009) Geochemistry of hypabyssal kimberlites from Lac de Gras, Canada: comparisons to a global database and applications to the parent magma problem. Lithos 112:236–248

Klein-BenDavid O, Pearson DG, Nowell GM, Ottley C, McNeill JCR, Logvinova A, Sobolev NV (2014) The sources and time-integrated evolution of diamond-forming fluids – trace elementsand isotopic evidence. Geochim Cosmochim Acta 125:146–169

Kopylova MG, Kostrovitsky SI, Egorov KN (2013) Salts in southern Yakutian kimberlites and the problem of primary alkali kimberlite melts. Earth Sci Rev 119:1–16

Kostrovitsky SI, Morikiyo T, Serov IV (2007) Isotope geochemical systematics of kimberlites and related rocks from the Siberian Platform. Russ Geol Geophys 48:272–290

Le Roex AP, Bell DR, Devis P (2003) Petrogenesis of group I kimberlites from Kimberley, South Africa: evidence from bulk-rock geochemistry. J Petrol 44:2261–2286

McDonough WF, Sun S-s (1995) The composition of the Earth. Chem Geol 120:223–253

Nikolaeva I, Palesskii S, Koz'menko O, Anoshin G (2008) Analysis of geologic reference materials for REE and HFSE by inductively coupled plasma-mass spectrometry (ICP-MS). Geochem Int 46: 1016–1022

Nishio Y, Nakai S, Yamamoto J, Sumino H, Matsumoto T, Prikhod'ko VS, Arai S (2004) Lithium isotopic systematics of the mantle-derived ultramafic xenoliths: implications for EM1 origin. Earth Planet Sci Lett 217:245–261

Nowell GM, Pearson DG, Bell DR, Carlson RW, Smith CB, Kempton PD, Noble SR (2004) Hf isotope systematics of kimberlites and their megacrysts: new constraints on their source regions. J Petrol 45: 1583–1612

Pokhilenko NP, Agashev AM, Litasov KD, Pokhilenko LN (2015) Carbonatite metasomatism of peridotite lithospheric mantle: implications for diamond formation and carbonatite-kimberlite magmatism. Russ Geol Geophys 56(1–2):280–295

Ringwood AE, Kesson SE, Hibberson W, Ware N (1992) Origin of kimberlites and related magmas. Earth Planet Sci Lett 113(4):521–538

Rosenthal A, Foley SF, Pearson DG, Nowell GM, Tappe S (2009) Petrogenesis of strongly alkaline primitive volcanic rocks at the propagating tip of the western branch of the East African Rift. Earth Planet Sci Lett 284:236–248

Smith CB (1983) Pb, Sr and Nd isotopic evidence for sources of southern African Cretaceous kimberlites. Nature 304:51–54

Smith CB, Gurney JJ, Skinner EMW, Clement CR, Ebrahim N (1985) Geochemical character of southern African kimberlites: a new approach based on isotopic constraints. Trans Geol Soc S Afr 88:267–280

Soltys A, Giuliani A, Phillips D, Kamenetsky VS, Maas R, Woodhead JD, Rodemann T (2016) In-situ assimilation of mantle minerals by

kimberlitic magmas - direct evidence from a garnet wehrlite xenolith entrained in the Bultfontein kimberlite (Kimberley, South Africa). Lithos 256–257:182–196

Sun J, Liu CZ, Tappe S, Kostrovitsky SI, Wu FY, Yakovlev D, Yang Y-H, Yang JH (2014) Repeated kimberlite magmatism beneath Yakutia and its relationship to Siberian flood volcanism: insights from in situ U-Pb and Sr-Nd perovskite isotope analysis. Earth Planet Sci Lett 404:283–295

Surgutanova EA, Agashev AM, Demonterova EI, Golovin AV, Pokhilenko NP (2016) Sr and Nd isotope composition of deformed peridotite xenoliths from Udachnaya kimberlite pipe. Dokl Earth Sci 471:1204–1207

Tainton KM, McKenzie D (1994) The generation of kimberlites, lamproites, and their source rocks. J Petrol 35:787–817

Tappe S, Pearson DG, Nowell G, Nielsen T, Milstead P, Muehlenbachs K (2011) A fresh isotopic look at Greenland kimberlites: cratonic mantle lithosphere imprint on deep source signal. Earth Planet Sci Lett 305:235–248

Tappe S, Kjarsgaard BA, Kurszlaukis S, Nowell GM, Phillips D (2014) Petrology and Nd-Hf isotope geochemistry of the Neoproterozoic Amon kimberlite sills, Baffin Island (Canada): evidence for deep mantle magmatic activity linked to supercontinent cycles. J Petrol 55:2003–2042

Tappe S, Brand NB, Stracke A, van Acken D, Liu C-Z, Strauss H, Wu F-Y, Luguet A, Mitchell RH (2017) Plates or plumes in the origin of kimberlites: U/Pb perovskite and Sr-Nd-Hf-Os-C-O isotope constraints from the Superior craton (Canada). Chem Geol 455:57–83

Taylor WR, Tomkins LA, Haggerty SE (1994) Comparative geochemistry of west African kimberlites: evidence for a micaceous kimberlite endmember of sublithospheric origin. Geochim Cosmochim Acta 58:4017–4037

Torsvik TH, Burke K, Steinberger B, Webb SJ, Ashwal LD (2010) Diamonds sampled by plumes from the core-mantle boundary. Nature 466:352–355

Vladimirov BM, Kostrovitsky SI, Solovieva LV, Botkunov AI, Fiveiskaya L, Egorov KN (1981) Classification of kimberlites and internal structure of kimberlite pipes. Nauka, Moscow, 131 pp (in Russian)

Weaver BL (1991) Trase element evidense for the origin of ocean-island basalts. Geology 19:123–126

Willbold M, Stracke A (2006) Trace element composition of mantle end-members: implications for recycling of oceanic and upper and lower continental crust. Geochem Geophys Geosyst 7(4):Q04004

Wilson MR, Kjarsgaard BA, Taylor B (2007) Stable isotope composition of magmatic and deuteric carbonate phases in hypabyssal kimberlite, Lac de Gras field, Northwest Territories, Canada. Chem Geol 242:435–454

Woodhead J, Hergt J, Phillips D, Paton C (2009) African kimberlites revisited: in situ Sr isotope analysis of groundmass perovskite. Lithos 112(S1):311–317

Yaxley GM, Berry AJ, Rosenthal A, Woodland AB, Paterson D (2017) Redox preconditioning deep cratonic lithosphere for kimberlite genesis – evidence from the central Slave Craton. Sci Rep-UK 7:30

Zindler A, Hart SR (1986) Chemical geodynamics. Annu Rev Earth Planet Sci 14:493–571